Coupled Systems Mechanics, *Vol. 4, No. 4 (2015) 297-316*
DOI: http://dx.doi.org/10.12989/csm.2015.4.4.297

Seismic fragility analysis of bridge response due to spatially varying ground motions

C. Kun*, B. Li and N. Chouw

The Department of Civil and Environmental Engineering, Faculty of Engineering, the University of Auckland, New Zealand

(Received July 22, 2015, Revised November 20, 2015, Accepted December 5, 2015)

Abstract. The use of fragility curves in the design of bridges is becoming common these days. In this study, experimental data have been used to develop fragility curves for the potential of girder unseating of a three-segment bridge and a bridge-abutment system including the influence of spatially varying ground motions, pounding, and abutment movement. The ground excitations were simulated based on the design spectra for different soil conditions. The Newmarket Viaduct replacement bridge in Auckland was used as the prototype bridge. These fragility curves were also applied to the 2010 Darfield and 2011 Christchurch earthquakes. The study showed that for bridges with similar characteristics as the chosen prototype and with similar fundamental frequencies, pounding could increase the probability of girder unseating by up to 35% and 30% based on the AASHTO and NZTA seating length requirements, respectively. The assumption of uniform ground excitations in many design practices, such as the NZTA requirements, could potentially be disastrous as girders might have a very good chance of unseating (as much as 53% higher chances when considering spatial variation of ground motions) even when they are designed not to. In the case of superstructures with dissimilar frequencies, the assumption of fixed abutments could significantly overestimate the girder unseating potential when pounding was ignored and underestimate the chances when pounding was considered. Bridges subjected to spatially varying ground excitations simulated based on the New Zealand design spectra for soft soil conditions with weak correlation shows the highest chances of girders falling off, of up to 65% greater than for shallow soil excitations.

Keywords: girder unseating; pounding; spatially varying ground motions; fragility curve; shake table testing

1. Introduction

Bridges are one of the most seismically vulnerable and important infrastructures in ensuring a functioning society. They are vital lifelines that are essential in providing access for rescue operations post-disasters. They provide access for the transportation of victims and supplies as well as search and rescue operations that are important in minimising casualties and loss of lives. Thus, it is crucial that their functionalities are maintained even after catastrophic events like earthquakes, volcano eruptions, and tsunamis.

Fragility curves are a common tool used in seismic design of structures nowadays especially for

*Corresponding author, Ph.D. Candidate, E-mail: ckun005@aucklanduni.ac.nz

http://www.techno-press.org/?journal=csm&subpage=7 ISSN: 2234-2184 (Print), 2234-2192 (Online)

conducting seismic risk assessments in moderate seismic zones. The increasing awareness in the vulnerability of structures in moderate seismic events was initiated by past earthquake events such as the 1989 Loma Prieta, 1994 Northridge, and 1995 Kobe earthquakes, where research and development on seismic risk assessments started to pick up (Ramanathan *et al.* 2011).

Fragility curves show the probability of a structure reaching or exceeding certain damage limit states at given intensity measures, normally the PGA or PGD in the case of earthquakes. They have been developed extensively but not limited to seismic events. Other than seismic fragility curves, they have also been developed for other disaster events such as tsunamis (Charvet *et al.* 2014, Weibe and Cox 2014), and windstorms (Gur and Ray-Chaudhuri 2013).

Plenty of fragility curves have been developed for masonry buildings and structural systems (Asteris *et al.* 2014, Lagomarsino and Cattari 2014), electric power stations (Cavalieri *et al.* 2014), water distribution pipelines (American Lifelines Alliance 2001) and bridges (Elnashai *et al.* 2004, Nielson and Desroches 2006, Pang *et al.* 2014). The importance of fragility curves in seismic design can be seen by their ability to provide a relation between the seismic hazard assessment of a particular site and the effects of the ground motions on the response of the structure. This information can provide a tool for prioritising retrofits, pre-earthquake planning, and estimation of losses (Nielson and Desroches 2003).

Fragility functions are particularly useful prior to the occurrence of earthquake events. They are usually used to predict the potential expected damage to structures and thus the socioeconomic effects, if said seismic events occur. These predictions are important in disaster planning because severe bridge damage could render them unusable for long periods of time, affecting or restricting transportation and rescue operations following earthquakes (Hwang *et al.* 2000a). An example of the usefulness in having better pre-disaster planning was in the 1994 Northridge earthquake, where Gordon *et al.* (1998) estimated a total of more than 1.5 billion dollars of economic losses due to disruption to the transportation system.

Fragility curves have typically been constructed using asset damage statistics from four main categories of sources (Rosetto *et al.* 2014):

- Post-earthquake surveys – Empirical fragility curves
- Expert elicitation – Expert elicitation fragility curves
- Simulated earthquakes – Analytical fragility curves
- Combination of the above – Hybrid fragility curves

Most existing fragility curves are empirical or analytical. Empirical fragility curves are normally considered the most reliable source of data because damage data used are real observations from past earthquakes. Many of these fragility curves were developed from damage data obtained from the 1994 Northridge earthquake (Basoz 1999) and 1995 Kobe earthquake (Shinozuka *et al.* 2000a). Analytical fragility curves are widely used due to the ease of development of ground motions numerically. Some of the analytical fragility curves developed are such as those by Shinozuka *et al.* (2000b) and Hwang *et al.* (2000b). Chao *et al.* (2015) also developed analytical fragility curves to investigate the seismic fragility of reinforced concrete bridges including chloride induced corrosion when subjected to spatially varying ground motions.

Although the reliability of fragility curves is improved because damage data from multiple events were used, the majority of fragility curves have been developed using damage data from single events (Rosetto *et al.* 2014), such as by Wiebe and Cox (2014) and Charvet *et al.* (2014) where fragility curves were developed for various structures based on the 2011 Great East Japan tsunami. These fragility curves are normally developed for structures with different classifications and characteristics.

Other than that, fragility curves were also developed using multiple ground excitations for structures of a single classification (i.e., similar characteristics). An example of this is the fragility curves developed by Shinozuka *et al.* (2000a), where the damage data used were obtained by subjecting the Memphis Bridge to multiple ground excitations.

Bridges are normally constructed so that adjacent spans have similar fundamental frequencies. This is a means of preventing girder unseating and pounding during earthquakes. However, bridge pounding inevitably occurs due to several reasons. One of them is the spatial variation of ground motions. This means that bridges designed to have similar fundamental frequencies will experience pounding or have relative opening displacements (Chouw and Hao 2005a, 2008a, b).

Furthermore, abutments are always more rigid than bridge segments. This means that the superstructures will have dissimilar fundamental frequencies. Thus, asynchronous movements between the segment and abutments will be unavoidable, even if the system experiences uniform ground motions.

The importance of considering spatial variation of ground motions has been recognised since the 1960s. Spatial variation of ground motions arise due to three main reasons, namely the wave passage effect, coherency loss effect, and site response effect.

Many investigations have been conducted on the influence of spatially varying ground motions on bridge responses, such as by Abdel-Ghaffar and Rubin (1982), Zerva (1991), Nazmy and Abdel-Ghaffar (1992), and Harichandran *et al.* (1996). Most of them have been conducted either numerically or analytically. Many of the earlier research works are without experimental validation.

Some of the experimental studies on the effects of pounding and spatially varying ground motions on bridge responses have been conducted by Crewe and Norman (2006) and Dryden (2009). However, construction of fragility curves using experimental data, to the author's best knowledge, has not yet been reported. Furthermore, investigations including multi-segment pounding are also scarce. Many studies investigating the effects of pounding only looked at one-sided pounding. In reality, bridges always experience two-sided pounding either with adjacent segments or with abutments.

Bridge-abutment pounding has also been investigated in the past. Some of these include the numerical investigations conducted by Won *et al.* (2008) and Weiser and Maragakis (2013). They highlighted the vulnerability of bridges unseating at the abutment expansion joint location.

In this study, fragility curves were developed by subjecting multiple ground motions. Based on the Newmarket Viaduct replacement bridge, a three-span bridge segment system and a bridge-abutment system are constructed. This paper presents the development of fragility curves using experimental data obtained through a series of shake table tests, focusing on the girder unseating potential. The effects of different soil classes, spatially varying ground motions and pounding on the girder unseating potential have been investigated. The effects of movable abutments will also be looked at. The specified seating lengths from some commonly adopted bridge design specifications (NZTA bridge manual, AASHTO specifications, and JRA specifications) will be compared.

2. Methodology

2.1 Model and setup

A scaled bridge system consisting of three identical spans and a bridge-abutment system were constructed based on one of the segments of the Newmarket Viaduct replacement bridge. The ground excitations were applied to the models using three uni-directional shake tables. Fig. 1 shows the model setup for the three-span bridge and bridge-abutment systems constructed.

The prototype used was one of the segments of the Newmarket Viaduct replacement bridge spanning 100 m, with a height of 15.5 m. The longitudinal fundamental frequency of the prototype was 0.98 Hz.

Similitude laws were applied to scale down the bridge. The bridge model made of Polyvinyl-chloride (PVC) spans 800 mm, and has a height of 124 mm. The dimensions of the piers were chosen so that the longitudinal fundamental frequency was scaled correctly to 1.96 Hz. Each pier was 21 mm wide and 3 mm thick. The seismic mass was scaled to 10.11 kg.

A more detailed description of the chosen bridge prototype, construction of bridge model, and testing and setup can be found from Li *et al.* (2012, 2013).

2.2 Fragility curve from experimental data

The fragility curves constructed in this investigation are based on data obtained from subjecting a bridge system consisting of three identical segments to uniform and spatially varying ground motions. The girder unseating potential based on minimum seating length requirements from the AASHTO and JRA specifications, and the NZTA Bridge Manual have been investigated.

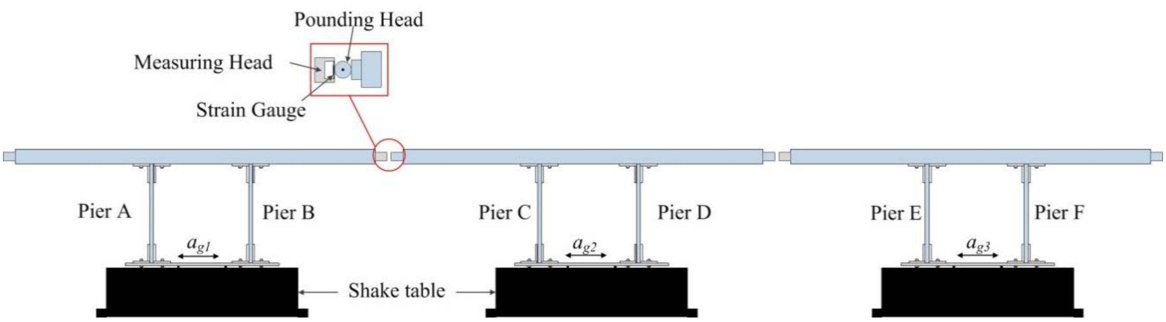

(a) Three-span bridge model

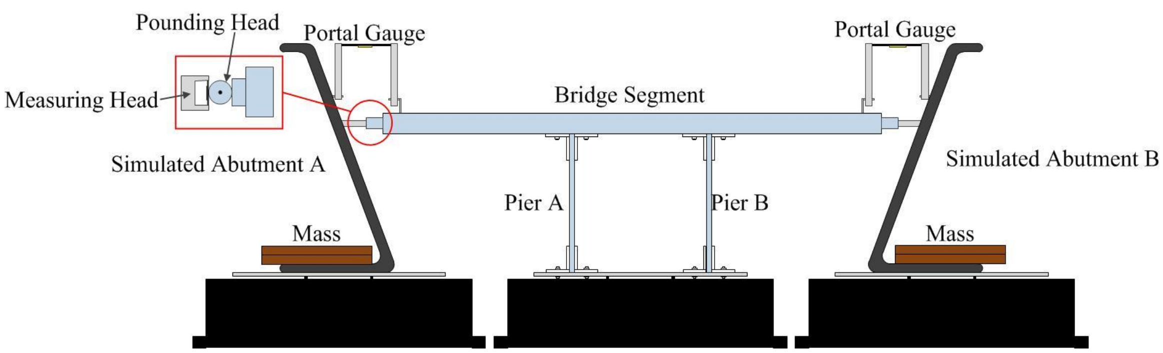

(b) Bridge-abutment system

Fig. 1 Test setup used

Conventional fragility curves are constructed by plotting the probability of exceeding certain damage states against intensity measures (Rosetto *et al.* 2014), expressed mathematically as

$$P(DS \geq ds_i \mid IM) \text{ for } IM_{\min} \leq IM \leq IM_{\max} \tag{1}$$

where DS is the damage experienced by the structure, ds_i is a predefined damage state, IM is the intensity measure chosen, usually Spectral Acceleration (S_a), Spectral Displacement (S_d), Peak Ground Acceleration (PGA), or Peak Ground Displacement (PGD), $P(DS \geq ds_i|IM)$ is the probability that the damage to a structure reaches or exceeds the given damage states, usually defined as:

i. no damage
ii. slight damage
iii. moderate damage
iv. extensive damage
v. complete damage/collapse

However, in this study a different approach is adopted, as the bridge models do not experience material nonlinearities, but subsequent damage potential due to pounding of adjacent structures and due to girder unseating, when subjected to the ground excitations. The probability of the girders unseating at specific PGDs was used, i.e.

$$P(d_{R,i} \geq SL_{\min,i} \mid PGD_i) \tag{2}$$

where $d_{R,i}$ is the girder opening relative displacement and $SL_{min,i}$ is the minimum seating length specified in the bridge design specification of interest at PGD_i.

2.3 Ground motions

The ground motions used in this study were stochastically simulated based on the New Zealand design spectra specified in NZS 1170.5 (Standards New Zealand, 2004). Ground motions for hard rock (Soil Class A), shallow soil (Soil Class C) and soft soil (Soil Class D) conditions have been simulated. The spatially varying ground motions for soft soil conditions (Soil Class D) were further split up into three categories: (i) highly correlated coherency (ii) intermediately correlated, and (iii) weakly correlated. The ground motions simulated for hard rock and shallow soil ground conditions were of highly correlated coherency. Further details on the ground motions simulated can be found in Li *et al.* (2012) and the numerical approach for simulating the ground motions can be found in Bi and Hao (2012).

The NZ target design spectra and response spectra of the simulated ground motions are shown for the three different soil conditions in Fig. 2. The vertical line marks the fundamental frequency of the prototype bridge adopted.

20 sets of ground motions have been developed for each soil class and coherency correlation. The influence of pounding between adjacent girders was investigated, where the initial gap size between the adjacent segments is zero. A comparison between the girder unseating potential based on the relative displacement between segments was made for with and without pounding effects.

Due to this linear, predictable behaviour of the bridge without pounding effects, the relative displacements obtained from 20 sets of each case were able to be scaled to specific PGDs (PGD_i = 50 mm, 100 mm, 150 mm etc.) to obtain more data for describing the probability of girder unseating. The relative displacements $R_{d,i}$ obtained were scaled by a PGD ratio

$$R_{d,i} = \frac{PGD_i}{PGD_{original}} \times R_{d,original} \tag{3}$$

where PGD_i is the PGD considered, $PGD_{original}$ is the PGD of the original ground motion, and $R_{d,original}$ is the corresponding relative displacement obtained at the original PGD value.

For example, if one of the ground motions originally had a PGD of 300 mm ($PGD_{original}$ = 300 mm) and the corresponding relative response obtained was 500 mm ($R_{d,original}$ = 500 mm), the relative response ($R_{d,i}$) at a PGD of 50 mm (PGD_i = 50 mm) will be

$$R_{d,50mm} = \frac{PGD_{50mm}}{PGD_{original}} \times R_{d,original}$$

$$R_{d,50mm} = \frac{50mm}{300mm} \times 500mm$$

$$R_{d,50mm} = 83.33mm$$

To investigate the effects of different soil conditions, the probability of girder unseating was plotted for each of the three soil conditions and the different coherency losses. Pounding was not included in the comparison of the different soil classes. Hence, the relative displacements can be scaled according to the scaling of the PGDs. The number of relative displacement data used to plot the probability of girder unseating at each PGD for each soil condition was 20 sets.

Lastly, the effects of spatial variation in ground motions have also been investigated. In this comparison, the probability of girder unseating without pounding was plotted for uniform and spatially varying ground motions, though it is clear that in the three-span bridge set up with uniform excitation, there is no out-of-phase movements and hence zero chances of girder unseating.

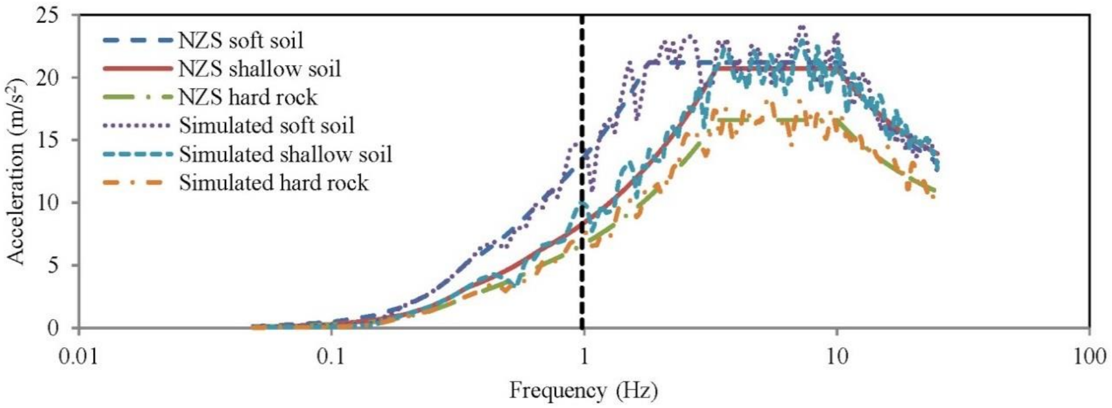

Fig. 2 Design and response spectra of simulated ground motions

2.4 Bridge design specifications

2.4.1 AASHTO specifications

AASHTO (2010) requires that bridges be designed for one of the four seismic design categories (SDC), A to D (refer to Clause 3.5, AASHTO specification). The specified minimum seating length, *SL* for all supports required for SDC A and B is shown in Eq. (4)

$$SL = 0.203 + 0.00167 L_s + 0.00666 H \tag{4}$$

where L_S is the span length in metres and *H* is the height of the column or pier in metres.

For SDC C and D, the minimum seating lengths for bridges are increased by a factor of safety of 1.5.

2.4.2 JRA specifications

The JRA (Japan Road Association, 2002) specifies that the seating length of girders, *S* shall be at least the minimum seating length, *SL* specified

$$S = u_{rel} + u_g \geq SL \tag{5}$$

$$SL = 0.7 + 0.005 l \tag{6}$$

$$u_g = \varepsilon_g L \tag{7}$$

where u_{rel} is the maximum relative displacement between adjacent structures when subjected to the strongest ground motions based on the Japanese design spectra; u_g is the relative displacement of the ground occurring due to ground deformation between piers; and *l* is the effective span length, in metres. For hard, medium and soft soil ε_g has the values of 0.0025, 0.00375 and 0.005, respectively. *L* is the distance between two substructures in metres. Although the seating length of girders includes the relative displacements between the adjacent structures, u_{rel} and the relative displacement of the ground between piers, u_g, which potentially accounts for the effects of spatially varying ground excitations, the minimum seating length requirement, *SL* was only dependent on the effective span length.

2.4.3 NZTA bridge manual

The required seating length, *SL* specified in the NZTA bridge manual (New Zealand Transport Agency, 2014) is given in Clause 5.5.2 (d) as

$$SL = 2E + 100\,mm \geq 400\,mm \tag{8}$$

where *E* is the relative movement between span and support.

It is noted that although some design specifications such as the EC8-2 accounts for the spatial variation of ground motions, Sextos and Kappos (2009) has found that it can still underestimate the actual seismic demand significantly. The AASHTO requirements for minimum girder seating length however, seem oversimplified due to it being governed only by the bridge span and pier height. On the other hand, the JRA provisions account for the influence of the frequency of neighbouring structures and spatial variation of ground motions through the relative movement between the adjacent structures, and the empirical relative ground movements at adjacent supports. Despite these considerations in the girder seating length, Chouw and Hao (2005b) has found that the JRA requirements could still underestimate the seating length required to prevent girder unseating. Lastly, the NZTA bridge manual requirements for the minimum girder seating length is dependant only on the relative displacement between span and support. Though the equation proposed by the NZTA provisions is intended to account for out-of-phase ground movements, it assumes only uniform ground excitations in the design of bridges, which could significantly underestimate the seating length as uniform ground motions result in little or no relative displacements.

3. Results and discussions

The minimum girder seating lengths were calculated based on the requirements specified in the AASHTO specifications, the JRA specifications, and the NZTA bridge manual.

The relative displacements obtained from the model testing have been scaled back to that expected for the prototype. The length scale factor of 125 was applied to the relative displacements to obtain the expected values experienced by the prototype bridge for suitable comparisons.

Based on Eq. (4), the minimum girder seating length specified in the AASHTO specifications is

$$SL = 0.203 + 0.00167 \times 100 + 0.00666 \times 15.5 = 0.47323m = 473.23mm$$

For JRA requirements, the minimum seating length is specified as

$$SL = 0.7 + 0.005 \times 100 = 1.2m = 1200mm$$

The minimum seating length specified in the NZTA bridge manual was 400 mm.

3.1 Effects of pounding and spatial variation of ground motions

A three-segment bridge model was subjected to uniform and spatially varying ground motions. In the cases where pounding was considered, the initial gap between the segments was zero. In the no pounding cases, they were spaced sufficiently apart to prevent contact.

Fig. 3 shows the probability of girder unseating with and without pounding during an earthquake based on (a) AASHTO, (b) JRA, and (c) NZTA specification requirements for minimum girder seating length, respectively when subjected to uniform and spatially varying ground motions. From Fig. 3, it can be seen that pounding tends to increase the likelihood of girder unseating for most PGD values for the AASHTO and NZTA requirements. The girder unseating potential based on the JRA provisions was almost zero across all PGDs. The chances of girder unseating started to occur past a PGD of 400 mm for the spatially varying excitation case without pounding.

Pounding reduces the chances of girder unseating only up to about 10% for the AASHTO requirements and less than 5% for the NZTA requirements at PGD less than 220 mm. The reductions occur only from 170 mm to 220 mm for the AASHTO requirements and from 130 mm to 200 mm for the NZTA requirements. However, at PGDs larger than these ranges, pounding tends to increase the likelihood of girder unseating by as much as 35% and 30% for the AASHTO and NZTA requirements, respectively.

The increase in girder relative displacement could potentially be due to the impact forces induced by collisions of the adjacent spans. Pounding could not only increase the girder unseating potential, as observed, it could also cause extensive localised damage at expansion joints of bridges, such as cracking and spalling of the concrete.

The JRA specifications on the other hand, being the most conservative (largest seating length requirement) amongst the design specifications of interest, shows zero chances of girder unseating for both with and without pounding within the range of PGDs investigated. This is because the seating length requirement based on the JRA specifications was almost 2.5 times larger than that of the AASHTO requirements, and 3 times larger than the NZTA requirements.

When subjected to uniform ground motions, the probability of girder unseating is always zero. This is not surprising because the bridge segments have identical characteristics and parameters and hence will move identically (i.e. no relative displacement) when subjected to uniform ground motions.

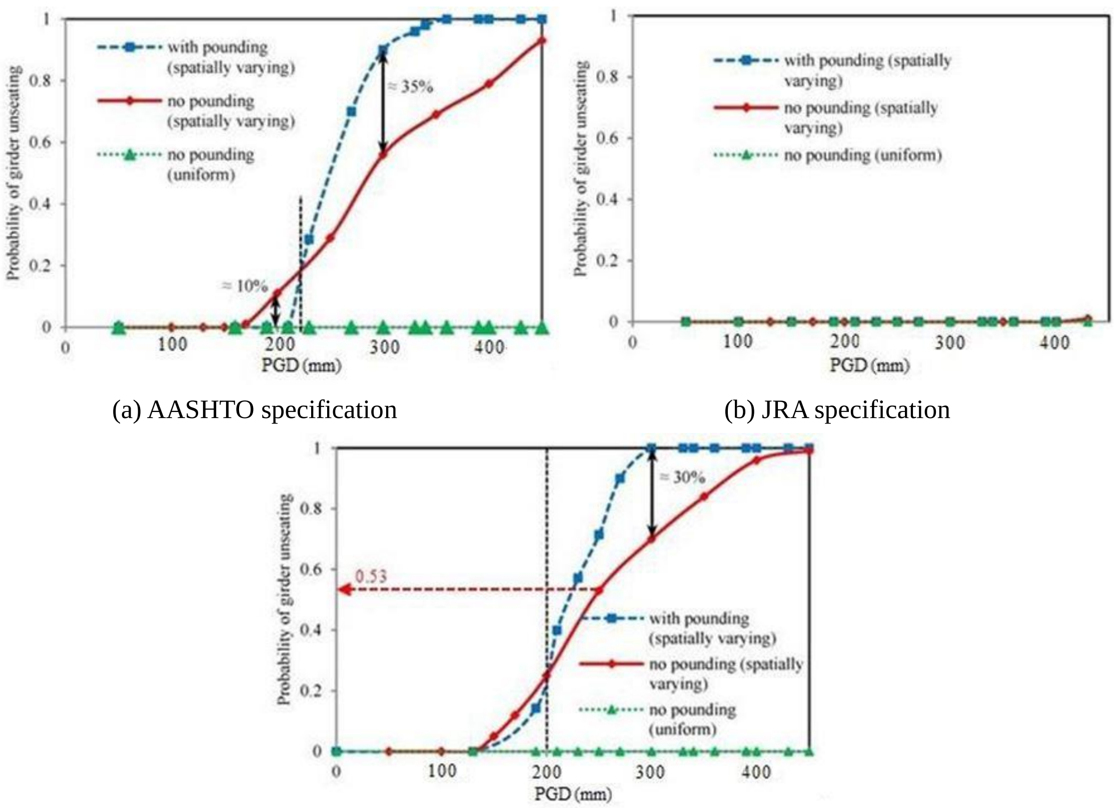

(a) AASHTO specification

(b) JRA specification

(c) NZTA specification

Fig. 3 Comparison of fragility curves of bridge girder unseating with and without pounding when subjected to uniform and spatially varying ground motions, excluding effects of ground motion characteristics and coherency loss, i.e. data for all cases considered are used

The assumption of uniform ground excitations adopted in the current NZTA design procedures significantly underestimates bridge girder unseating potential. From Fig. 3(c), the girder unseating potential at a relatively moderate PGD of 250 mm for spatially varying ground motions without pounding is 53%, but based on the assumption of uniform ground motions, there is zero chances of girder unseating happening at the same PGD. This shows the significance of incorporating spatial variation of ground motions in current design procedures.

3.2 Effect of abutment movement

The effects of abutment movement on the girder unseating potential will be discussed in this section. Fig. 4 shows the fragility curves developed for the bridge-abutment model based on the AASHTO, JRA, and NZTA design requirements for girder seating length. Design guidelines do not normally take into account abutment movement when considering the girder seating length. This section looks at the consequences of assuming fixed abutments and that of considering abutment movement.

From Fig. 4, we can see that the JRA requirements are again much more conservative than the AASHTO and NZTA requirements. In the range of PGDs considered, based on the JRA requirements for girder seating length, bridges will not experience girder unseating.

For the AASHTO and NZTA requirements, it can be seen that the assumption of fixed abutments and no pounding between the bridge segment and abutments has the highest chances of occurrence of girder unseating in the range of PGDs considered. The chances of girder unseating occurring started at a PGD of as small as 100 mm. On the other hand, when the abutments were assumed to be fixed, and pounding was considered, the girder unseating potential was zero in the range of PGDs considered. This was because the abutments essentially restrict any movement of the bridge segment.

In reality, fixed abutments do not occur during earthquakes. They will always be excited along with the bridge segment. From Fig. 4, it can be seen that the fragility curve for the cases when the bridge-abutment system was subjected to uniform and spatially varying ground motions were quite similar. In the case of spatially varying ground motions, the girder unseating potential generally tends to be slightly higher compared to uniform excitations.

The assumption of fixed abutments and excluding the effects of pounding could potentially lead to significant overestimation of the girder unseating potential compared to the more realistic case when abutment movements are allowed and pounding was considered. In the case of the AASHTO requirements, a potential 52% overestimation compared to the uniform excitation and spatially varying excitation considering pounding could be seen. Based on the NZTA requirements, the assumption could lead to a potential 58% and 63% overestimation of the maximum percentage increment of girder unseating potential for the uniform and spatially varying excitations, respectively. This means that bridges designed based on these assumptions could be uneconomical and too conservative. On the other hand, if the assumption of fixed abutments was adopted and pounding was included, the design will be severely underestimating the girder unseating potential compared to movable abutments with pounding, leading to unsafe designs. It is noted that although there was no chance of girder unseating occurrence for the case of fixed abutments considering pounding. In this study, fixed abutments are assumed for simplicity. In reality, adjacent abutments move with the ground during earthquake events, thus may potentially increase the relative displacements between the superstructures, and consequently the potential of girder unseating. The fixed abutments in this study provided significant restrictions to the movement of the bridge segment, thus limiting its girder unseating potential.

Because of the assumption of moving abutments (both uniform and spatially varying excitations), the fragility curves were in between that of the fixed abutment cases. This is because in the case where abutments were allowed to move, they still provided restrictions to the relative displacements, thus the girder has lower chances of unseating occurring compared to the fixed abutments case without pounding. The case with movable abutments have higher chances of girder unseating compared to the fixed abutments case with pounding because the latter provides more restriction.

For both the AASHTO and NZTA requirements, the chances of girder unseating occurring was higher for the case with spatially varying excitations compared to the uniform excitations for PGD larger than 400 mm. This means that for PGDs above 400 mm, the effects of spatially varying excitations on causing out-of-phase movements is more pronounced.

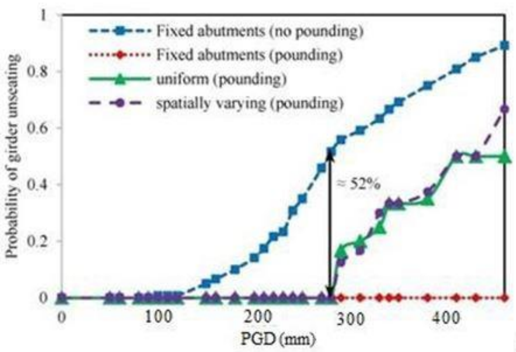

(a) AASHTO specification

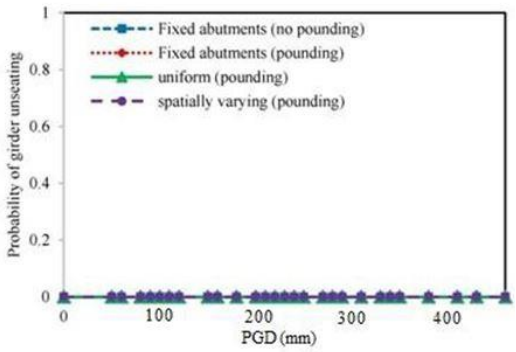

(b) JRA specification

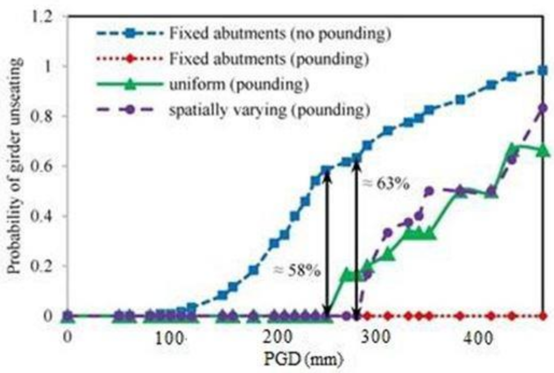

(c) NZTA specification

Fig. 4 Comparison of effects of abutment movement on girder unseating for various design specifications, excluding effects of ground motion characteristics and coherency loss, i.e., data for all cases considered are used

3.3 Effects of soil conditions and coherency loss for various design specifications

The influence of soil conditions on the girder unseating potential has also been investigated. The ground motions were spatially varying and pounding was not included. In this section, a comparison of the likelihood of girder unseating when the three-span bridge model was subjected to ground motions developed based on various soil conditions (soft soil - strong, intermediate, and weak correlation, shallow soil- strong correlation, and hard rock – strong correlation) will be discussed. The results for the three design specifications of interest will also be compared.

First looking at the different design specifications, from Fig. 5, it can clearly be seen that the fragility curves for the JRA requirement is not as steep as the AASHTO and NZTA requirements due to the larger minimum seating length specified.

For the AASHTO requirements, girder unseating tends to start to occur at PGD of around 150 – 170 mm for soft and shallow soil conditions, respectively, whereas for the hard rock conditions girder unseating starts occurring at a larger PGD of around 200 mm. A 100% occurrence of girder unseating based on the AASHTO requirements ranges from a PGD of as low as 400 mm (soft soil –weak correlation) to as high as 600 mm (shallow soil).

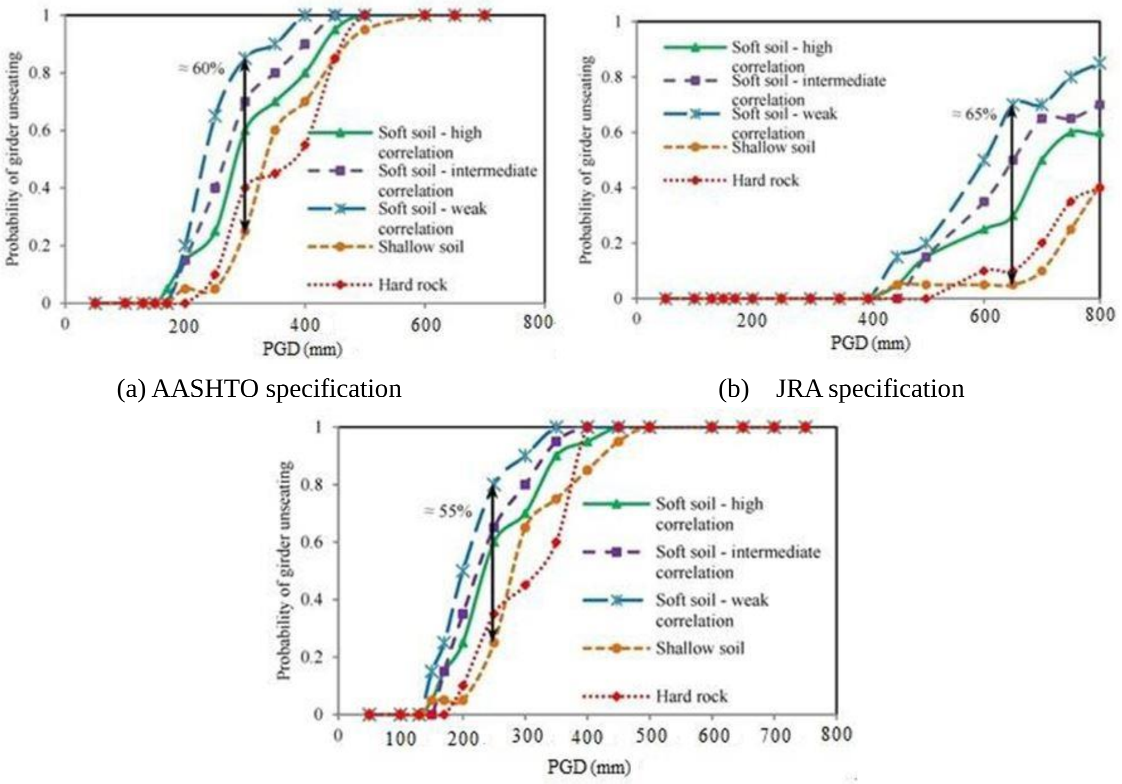

(a) AASHTO specification (b) JRA specification

(c) NZTA specification

Fig. 5 Fragility curves of bridge for ground excitations based on various soil conditions without considering pounding

On the other hand, for the NZTA requirements, girder unseating starts to occur at PGD of around 130 – 150 mm for soft and shallow soil conditions, and at PGD of around 170 mm for hard rock conditions. Girder unseating has a 100% chance of occurring at PGD of 350 mm to 500 mm. Unsurprisingly, the JRA requirements for seating length are much more conservative than the other specifications, girder unseating only starts to occur at PGDs of 400 – 500 mm.

For all three design specifications, it is evident that the bridge has the largest chances of experiencing girder unseating when subjected to soft soil ground motions compared to shallow soil or hard rock conditions. The chances of girder unseating of the bridge tend to be similar when subjected to the shallow soil and hard rock excitations.

Fig. 5(a) shows that the range of PGDs that could potentially cause girder unseating is the smallest (between 150 mm and 400 mm) when subjected to weakly correlated soft soil ground motions. For the other soil types where the correlation is higher, for example the shallow soil excitation, the range of PGDs where girder unseating potentially occurs tends to be larger (from 170 mm to 600 mm).

It can also be deduced from Fig. 5 that although the JRA design specifications give the most conservative probability of girder unseating overall, bridges subjected to weakly correlated soft soil excitations could see a maximum increase in chances of girder unseating of up to 65% than when subjected to shallow soil excitations, whereas for the AASHTO and NZTA specifications, the maximum percentage increment of chances of girder unseating increased only by as much as 60% and 55%, respectively when the same comparison was made.

3.4 Application of fragility curve in 2010 Darfield and 2011 Christchurch earthquakes

In this section, the chance of occurrence of girder unseating of bridges with similar characteristics as the prototype of interest is discussed. An example of how the fragility curves developed in earlier sections can be applied in seismic events is discussed. The September 2010 Darfield and February 2011 Christchurch earthquakes will be used as an example in this study. The fragility curves developed based on the NZTA bridge manual requirements for girder seating length will be used in this discussion.

The PGDs recorded at the various stations during the aforementioned seismic events is shown in Tables 1 and 2.

3.4.1 Likelihood of girder unseating with and without pounding

From the Darfield Earthquake, assuming that bridges experience spatially varying ground motions and pounding does not occur, according to Fig. 3(c), bridges with similar characteristics as the one used in this study will have at least a 53% chance (PGD $\geq$ 250 mm) of girders unseating at 21 out of the 70 stations (30%) where the ground excitations were recorded, such as the CACS, CBGS, and CCCC stations. From the 21 stations, bridges built at around 90% (19 out of the 21 stations) of the areas will have a 70% chance of girders falling off (PGD $\geq$ 300 mm).

However, when pounding was incorporated, at PGD $\geq$ 250 mm, the likelihood of girder unseating was increased to at least about 71% for the 21 stations, and the bridges built near the 19 stations will see an increase in chances of girder unseating from 70% to 100%. This means that the consequences of not considering pounding in bridge design could potentially be disastrous.

On the other hand, in the Christchurch Earthquake event that occurred in February 2011, assuming pounding between adjacent bridges do not occur, from Fig. 3(c), bridges have at least a 53% chance of girders falling (PGD $\geq$ 250 mm) in areas near 7 of the 45 stations (about 16%)

where the ground motions were recorded, such as the NNBS and REHS stations. Although out of the 7 stations, none of them have 100% chances of girders falling off (PGD > 450 mm), 6 of them will have at least a 70% chance (PGD ≥ 300 mm) of occurrence.

When pounding was incorporated, the chances of girder unseating at the 7 areas was again increased from 53% to 71%, with 100% chance of girder unseating occurring when PGD exceeds 300 mm.

Table 1 PGD and soil classes recorded at 70 stations during the September 2010 Darfield Earthquake (GeoNet – Darfield Earthquake)

Station	Soil Class	PGD (mm)	Station	Soil Class	PGD (mm)	Station	Soil Class	PGD (mm)
ADCS	D	98.46	HPSC	N/A	437.2	RDCS	D	44.765
APPS	C	17.061	HSES	D	56.981	REHS	D	524.3
ARPS	B	19.954	HVSC	N/A	152.2	RHSC	N/A	363.5
ASHS	D	67.351	IFPS	D	25.979	RKAC	D	183.9
AVIS	B	20.308	INGS	C	41.212	ROLC	D	539.6
BENS	B	13.313	KHZ	B	31.89	RPZ	B	29.921
CACS	D	452	KIKS	B	39.284	SBRC	D	308.2
CBGS	D	285.7	KOKS	D	27.989	SHLC	N/A	454.5
CCCC	D	458.5	KPOC	N/A	341.5	SJFS	D	58.658
CECS	C	50.071	LINC	D	664.5	SMTC	N/A	445.7
CHHC	D	532.1	LPCC	B	179.6	SPFS	D	60.572
CMHS	D	302.6	LRSC	D	120.8	SWNC	D	224.7
CSHS	B	57.516	LSRC	C	105.6	TKAS	B	19.166
DFHS	D	241.1	LTZ	B	86.808	TPLC	D	767.6
DORC	D	90.5	MAYC	D	60.495	TRCS	C	51.754
DSLC	D	491.3	MCAS	D	58.282	TWAS	D	17.908
FDCS	D	34.877	MCNS	N/A	18.696	WAKC	C	80.667
FGPS	D	41.854	MOLS	B	26.447	WSFC	D	69.209
FJDS	D	34.958	NNBS	E	247.1	WTMC	C	62.819
GDLC	D	726.9	OAMS	C	26.904	WVAS	D	43.553
GMTS	D	24.595	PEEC	C	33.142	WVZ	B	34.644
HAFS	D	64.237	PKIS	B	18.18	Q10503E01	N/A	456
HMCS	D	38.587	PPHS	D	475.4			
HORC	D	460.2	PRPC	E	259.8			

Table 2 PGD recorded at 45 stations during the February 2011 Christchurch Earthquake (GeoNet – Christchurch Earthquake)

Station	Soil Class	PGD (mm)	Station	Soil Class	PGD (mm)
ADCS	D	11.236	LPCC	B	115.3
AMBC	D	22.167	LSRC	C	14.493
ASHS	D	29.996	LTZ	B	10.228
CACS	D	100.5	NNBS	E	302.1
CBGS	D	216.4	PPHS	D	205.3
CCCC	D	223.3	PRPC	E	386.2
CECS	C	6.808	REHS	D	253.2
CHHC	D	215.1	RHSC	N/A	79.1
CMHS	D	121.8	RKAC	D	21.842
CSHS	B	8.244	ROLC	D	48.287
CSTC	D	19.607	SBRC	D	28.707
D06C	N/A	102.1	SCAC	B	6.156
D08C	N/A	405.6	SHFC	C	8.717
D09C	N/A	339.4	SHLC	N/A	305.7
DFHS	D	17.551	SLRC	N/A	33.09
DORC	D	18.265	SMTC	N/A	136.8
DSLC	D	37.376	SPFS	D	8.056
HORC	D	16.326	SWNC	D	52.401
HPSC	N/A	433.8	TPLC	D	74.084
HVSC	N/A	230.2	WAKC	C	14.706
KOWC	D	9.916	WIGC	C	7.935
KPOC	N/A	112.1	WSFC	D	8.581
LINC	D	85.271			

3.4.2 Likelihood of girder unseating for excitations based on different soil conditions

The fragility curves developed for the different soil conditions were also applied to the data from the Darfield and Christchurch earthquakes. It is noted that for the soft and very soft soil conditions (Soil Class D and E), only the fragility curve with high correlation was used. Pounding was not considered in this comparison. The fragility curves are shown in Fig. 6.

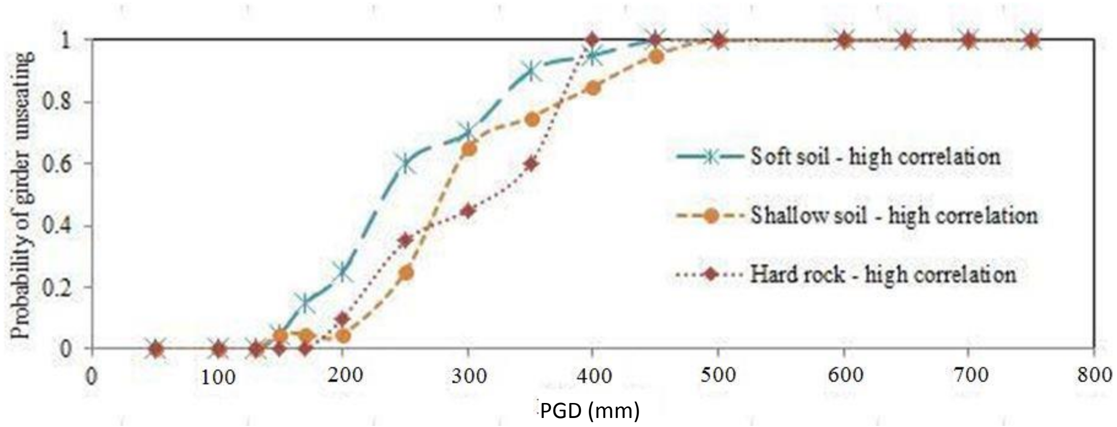

Fig. 6 Fragility curves for soft soil - highly correlated, shallow soil, and hard rock conditions based on the NZTA bridge manual requirements

For the Darfield Earthquake, there were 13 stations with hard rock conditions, 9 with shallow soil conditions, and 40 with soft soil conditions, whereas for the Christchurch Earthquake, there were 4 stations with hard rock conditions, 5 with shallow soil conditions, and 26 with soft soil conditions.

From the data recorded during the Darfield event, the recorded PGDs for hard rock conditions were mostly between 20 and 40 mm, with the exception of a 179.6 mm PGD recorded at the LPCC station. This means that in areas with hard rock conditions, the chances of girder unseating are generally minimal. Only bridges at areas near the LPCC station will have about a 3.2% chance (interpolated) of girder unseating.

For the shallow soil conditions (Soil Class C), the PGDs recorded were generally between 10 and 60 mm, with the exception of a 105.6 mm recorded at the LSRC station. However, from Fig. 6, it can be seen that in the worst case of sites with shallow soil condition (PGD = 105.6 mm), there is still no chance for girder unseating to occur. This means that even during a strong earthquake (Richter magnitude of 6.3), areas with shallow soil and hard rock conditions generally have small PGDs, and thus minimal observations of bridge girder unseating.

15 of the 40 stations with soft soil conditions recorded PGDs of at least 250 mm. Assuming ground motions are weakly correlated, this means that bridges in these areas have at least at 60% chance of girder unseating occurring during the Darfield event. Out of the 15 stations, 13 of them (about 87%) had at least 70% chance of girder unseating (PGD $\geq$ 300 mm) happening to bridges with similar characteristics in the nearby areas.

In the Christchurch Earthquake, 3 of the 4 stations with hard rock conditions recorded PGDs of less than 20 mm, and the other (LPCC station) recorded a PGD of 115.3 mm. However from Fig. 6, it can be seen that there is still no chance of girder unseating happening even for bridges near the LPCC station. It is also certain that there will be no girder unseating happening in areas near the shallow soil sites because from Table 2, the recorded PGDs for Soil Class C tends to be less than 20 mm.

Lastly, for stations with soft soil conditions, 2 of the 26 stations recorded PGDs of at least 300 mm. This means that bridges built in these areas will have at least 70% chance of girder unseating.

It is noted once again that these observations are only applicable to bridges that have similar characteristics as the prototype considered.

4. Conclusions

This paper presented the construction of fragility curves for a bridge structure through experimental work, focusing on the girder unseating potential. The Newmarket Viaduct replacement bridge was used as the prototype. A three-span bridge model and a bridge-abutment model was constructed and subjected to a series of shake table tests. The probability of girder unseating when subjected to spatially varying ground motions and including the effects of pounding was discussed. The effects of different soil conditions on the girder unseating potential were also investigated. These fragility curves were applied to the September 2010 Darfield and February 2011 Christchurch earthquakes to look at the potential of girder unseating happening to bridges with similar characteristics during these events. This study reveals that:

- Pounding inevitably occurs during seismic events due to out-of-phase movements caused by spatial variations in ground motions or adjacent structures having dissimilar fundamental natural frequencies, thus matching the fundamental frequencies of adjacent bridges will often be insufficient.
- For the three-segment bridge system (adjacent segments with similar fundamental frequencies),
    - Two-sided pounding tends to increase the chances of girder unseating occurring at larger PGDs due to the higher energy gain caused by the impact actions.
    - The assumption of uniform ground motions adopted in many current bridge design specifications for minimum bridge girder seating lengths, such as the NZTA bridge manual could significantly underestimate the actual required seating length.
    - Ground motions simulated based on the New Zealand soft soil design spectrum with weak correlations causes the worst girder unseating potential based on the fragility curves developed. Those subjected to the shallow soil and hard rock ground excitations generally have lower chances of girders falling off.
    - The fragility curves for the shallow soil and hard rock excitations have shallower slopes than that of the soft soil excitations. This means that the chances of girder unseating occurring tend to increase at a slower rate than the soft soil excitations.
- For the bridge-abutment system (superstructures with dissimilar fundamental frequencies),
    - The assumption of fixed abutments could significantly overestimate or underestimate the bridge girder unseating potential, depending on whether pounding was considered.
    - When pounding was considered, the abutments essentially restrict the bridge movement, thus the girder unseating potential will be significantly underestimated.
    - On the other hand, when pounding was ignored, the girder unseating potential was found to be potentially overestimated. This could lead to uneconomical designs.
    - When the abutments were subjected to uniform and spatially varying ground excitations, the fragility curves developed were quite similar, although the one for spatially varying ground motions tend to have slightly larger chances of occurrence of girder unseating.

- The Darfield and Christchurch earthquakes were used as an example of the application of the fragility curves developed in seismic events. It is noted that the fragility curves are only applicable to bridges with similar characteristics. For more accurate results, other factors such as the effects of soil-structure interaction (SSI) and the inelastic response of the bridge need to be incorporated.

Acknowledgments

The authors would like to thank the Ministry of Business, Innovation, and Employment for the support through the Natural Hazards Research Platform under the Award 907213701868.

References

AASHTO (2010), *Load and resistance factor design (LRFD) specifications for highway bridges,* American Association of State Highway and Transportation Officials, Washington D.C., USA.

Abdel-Ghaffar, A.M. and Rubin, L.I. (1982), "Suspension bridge response to multiple-support excitations", *J. Eng. Mech.Division*, **108**(2), 419-435.

American Lifelines Alliance (2001), "Seismic fragility formulations for water systems, Part 1: Guidelines", American Society of Civil Engineers (ASCE) and Federal Emergency Management Agency (FEMA). Retrieved from http://www.americanlifelinesalliance.com/pdf/Part_1_Guideline.pdf

Asteris, P.G., Chronopoulos, M.P., Chrysostomou, C.Z., Varum, H., Plevris, V., Kyriakides, N. and Silva, V. (2014), "Seismic vulnerability assessment of historical masonry structural systems", *Eng. Struct.*, **62-63**, 118-134.

Basoz, N.I. (1999), "Statistical analysis of bridge damage data from the 1994 Northridge, CA, earthquake", *Earthq.Spectra*, **15**(1), 25-54.

Bi, K. and Hao, H. (2012), "Modelling and simulation of spatially varying earthquake ground motions at sites with varying conditions", *Probabilist. Eng. Mech.*, **29**, 92-104.

Cavalieri, F., Franchin, P. and Pinto, P.E. (2014), "Fragility functions of electric power stations", *SYNER-G: Typology Definition and Fragility Functions for Physical Elements at Seismic Risk,* **27**, 157-185, Springer, Netherlands.

Charvet, I., Ioannou, I., Rossetto, T., Suppasri, A. and Imamura, F. (2014), "Empirical fragility assessment of buildings affected by the 2011 Great East Japan tsunami using improved statistical models", *Nat. Hazards*, **73**(2), 951-973.

Chouw, N. and Hao, H. (2005a), "Study of SSI and non-uniform ground motion effect on pounding between bridge girders", *Soil Dyn. Earthq. Eng*., **25**, 717-728.

Chouw, N. and Hao, H. (2005b), "Evaluation of adequacy of Japanese code specifications on required bridge girders seating", *Proceedings of the Australian Structural Engineering Conf.,* Newcastle, 11-14 September.

Chouw, N. and Hao, H. (2008a), "Significance of SSI and non-uniform near-fault ground motions in bridge response II: Effect on response with modular expansion joint", *Eng. Struct.*, **30**, 154-162.

Chouw, N. and Hao, H. (2008b), "Significance of SSI and non-uniform near-fault ground motions in bridge response I: Effect on response with conventional girder gap", *Eng. Struct.*, **30**, 141-153.

Chouw, N., Hao, H. and Su, H. (2006), "Multi-sided pounding response of bridge structures with non-linear bearings to spatially varying ground excitation", *Adv. Struct. Eng.*, **9**(1), 55-66.

Crewe, A.J. and Norman, A.J.P. (2006), "Experimental modelling of multiple support excitations of long span bridges", *Paper presented at the 4th International Conference on Earthquake Engineering*, Taipei, October.

Dryden, G.M. (2009), *The Integration of Experimental and Simulation Data in the Study of Reinforced Concrete Bridge Systems Including Soil-Foundation-Structure Interaction*, University of California, Berkeley, California, USA.

Elnashai, A.S., Borzi, B. and Vlachos, S. (2004), "Deformation-based vulnerability functions for RC bridges", *Struct. Eng. Mech.*, **17**(2), 215-244.

GeoNet - Christchurch Earthquake. Strong Motion FTP Site (2011), ftp://ftp.geonet.org.nz/strong/processed/Proc/2011/02_Christchurch_mainshock_extended_pass_band/

GeoNet - Darfield Earthquake. Strong Motion FTP Site (2010), ftp://ftp.geonet.org.nz/strong/processed/Proc/2010/09_Darfield_mainshock_extended_pass_band/

Gordon, P., Richardson, H. and Davis, B. (1998), "Transport-related impacts of the Northridge earthquake", *J. Transportation and Statistics*, **1**(2), 21-36.

Gur, S. and Ray-Chaudhuri, S. (2013), "Vulnerability assessment of container cranes under stochastic wind loading", *Struct. Infrastruct. E.*, **10**(12), 1511-1530. doi: 10.1080/15732479.2013.834943.

Harichandran, R.S., Hawwari, A. and Sweidan, B.N. (1996), "Response of long-span bridges to spatially varying ground motion", *J. Struct. Eng. - ASCE*, **122**(5), 476-484.

Hwang, H., Jernigan, J.B., Billings, S. and Werner, S.D. (2000a), "Expert opinion survey on bridge repair strategy and traffic impact", *Proceedings of the Post Earthquake Highway Response and Recovery Seminar*, St Louis, Missouri, September.

Hwang, H., Jernigan, J.B. and Lin, Y.W. (2000b), "Evaluation of seismic damage to Memphis bridges and highway systems", *J. Bridge Eng.*, **5**(4), 322-330.

Japan Road Association (2002), "Design Specifications for Highway Bridges", Tokyo, Japan.

Lagomarsino, S. and Cattari, S. (2014), "Fragility functions of masonry buildings", *SYNER-G: Typology Definition and Fragility Functions for Physical Elements at Seismic Risk*, **27**, 111-156, Springer, Netherlands.

Li, B., Bi, K., Chouw, N., Butterworth, J.W. and Hao, H. (2012), "Experimental investigation of spatially varying effect of ground motions on bridge pounding", *Earthq. Eng. Struct. D.*, **41**(14), 1959-1976.

Li, B., Bi, K., Chouw, N., Butterworth, J.W. and Hao, H. (2013), "Effect of abutment excitation on bridge pounding", *Eng. Struct.*, **54**, 57-68.

Chao, L., Hao, H., Li, H. and Bi, K. (2015), "Seismic fragility analysis of reinforced concrete bridges with chloride induced corrosion subjected to spatially varying ground motions", *Int. J. Struct. Stability Dynam.*, **16**, 1550010-1 – 1550010-27. doi: 10.1142/S0219455415500108.

Nazmy, A.S. and Abdel-Ghaffar, A.M. (1992), "Effects of ground motion spatial variability on the response of cable-stayed bridges", *Earthq. Eng. Struct. D.*, **21**(1), 1-20.

New Zealand Transport Agency (2014), "Bridge Manual (SP/M/022)", Wellington, New Zealand.

Nielson, B. and Desroches, R. (2003), "Seismic fragility curves for bridges: A tool for retrofit prioritization", *Proceedings of the 6th US Conference and Workshop on Lifeline Earthquake Engineering*, 1060-1070, Long Beach, California, August.

Nielson, B.G. and Desroches, R. (2006), "Seismic fragility methodology for highway bridges", *Paper presented at the Structures Congress*, St Louis, Missouri, May.

Pang, Y., Wu, X., Shen, G. and Yuan, W. (2014), "Seismic fragility analysis of cable-stayed bridges considering different sources of uncertainties", *J. Bridge Eng.*, **19**(4).

Ramanathan, K., Padgett, J.E. and Desroches, R. (2011), "Fragility curves for typical multispan simply supported bridge classes in moderate seismic zones: Pre- and post-seismic design considerations", *Proceedings of the 3rd ECCOMAS Thematic Conference on Computational Methods in Structural Dynamics and Earthquake Engineering*, Corfu, Greece, May.

Rossetto, T., D'Ayala, D., Ioannou, I. and Meslem, A. (2014), "Evaluation of existing fragility curves", *SYNER-G: Typology Definition and Fragility Functions for Physical Elements at Seismic Risk*, **27**, 47-93, Springer, Netherlands.

Sextos, A.G. and Kappos, A.J. (2009), "Evaluation of seismic response of bridges under asynchronous excitation and comparisons with Eurocode 8-2 provisions", *Bull. Earthq. Eng.*, **7**(2), 519-545.

Shinozuka, M., Feng, M.Q., Kim, H.K. and Kim, S.H. (2000b), “Nonlinear static procedure for fragility curve development”, *J. Eng. Mech. - ASCE*, **126**(12), 1287-1296.

Shinozuka, M., Feng, M.Q., Lee, J. and Naganuma, T. (2000a), “Statistical analysis of fragility curves”, *J. Eng. Mech. - ASCE*, **126**(12), 1224-1231.

Standards New Zealand Technical Committee (2004), “Structural design actions Part 5: Earthquake actions - New Zealand” (NZS 1170.5: 2004), Wellington, New Zealand.

Weiser, J. and Maragakis, M. (2013), “Seismic performance of highway bridges with seat-type abutments subjected to near-fault ground motions”, *Proceedings of the 2013 Structures Congress*, 827-838, Pittsburgh, Pennsylvania, May.

Wiebe, D.M. and Cox, D.T. (2014), “Application of fragility curves to estimate building damage and economic loss at a community scale: A case study of Seaside, Oregon”, *Nat. Hazards*, **71**(3), 2043-2061.

Won, J., Mha, H., Cho, K. and Kim, S. (2008), “Effects of the restrainer upon bridge motions under seismic excitations”, *Eng. Struct.*, **30**(12), 3532–3544.

Zerva, A. (1991), “Effect of spatial variability and propagation of seismic ground motions on the response of multiply supported structures”, *Probabilist. Eng. Mech.*, **6**(3), 212-221.